19. Ledentsov, N. N. *et al.* Quantum-dot heterostructure lasers. *IEEE J. Select. Top. Quant. Electron.* **6**, 439–451 (2000).

20. Chuang, S. L. *Physics of Optoelectronic Devices* (Wiley-Interscience, New York, 1995).

21. Painter, O. *et al.* Two-dimensional photonic band-gap defect mode laser. *Science* **284**, 1819–1821 (1999).

22. Ryu, H.-Y. *et al.* Square-lattice photonic band-gap single-cell laser operating in the lowest-order whispering gallery mode. *Appl. Phys. Lett.* **80**, 3883–3885 (2002).

....

Prolonged KREEP magmatism on the Moon indicated by the youngest dated lunar igneous rock

Lars E. Borg[1], **Charles K. Shearer**[1], **Yemane Asmerom**[2] & **James J. Papike**[1]

[1]*Institute of Meteoritics, Department of Earth and Planetary Sciences, and* [2]*Department of Earth and Planetary Sciences, University of New Mexico, Albuquerque, New Mexico 87131, USA*

....

Primordial solidification of the Moon (or its uppermost layer) resulted in the formation of a variety of rock types that subsequently melted and mixed to produce the compositional diversity observed in the lunar sample suite[1,2]. The initial rocks to crystallize from this Moon-wide molten layer (the magma ocean) contained olivine and pyroxene and were compositionally less evolved than the plagioclase-rich rocks that followed. The last stage of crystallization, representing the last few per cent of the magma ocean, produced materials that are strongly enriched in incompatible elements including potassium (K), the rare earth elements (REE) and phosphorus (P)—termed KREEP[3–5]. The decay of radioactive elements in KREEP, such as uranium and thorium, is generally thought to provide the thermal energy necessary for more recent lunar magmatism[4,6,7]. The ages of KREEP-rich samples are, however, confined to the earliest periods of lunar magmatism between 3.8 and 4.6 billion years (Gyr) ago[8,9], providing no physical evidence that KREEP is directly involved in more recent lunar magmatism. But here we present evidence that KREEP magmatism extended for an additional 1 Gyr, based on analyses of the youngest dated lunar sample.

Northwest Africa 773 (NWA 773) is a 633-g lunar meteorite composed of an impact breccia. The bulk of the sample is an olivine cumulate clast that is interpreted to be of igneous origin[10,11]. The clast contains approximately 48% olivine, 27% pigeonite, 11% augite, 2% hypersthene, and 11% plagioclase, as well as a mesostasis component characterized by trace amounts of barian K-feldspar, merrillite, troilite, Cr-spinel, and Fe–Ni metal. In addition to these igneous phases, NWA 773 contains secondary alteration products that were added to the meteorite during terrestrial weathering in the African desert. The composition of both the bulk sample and parental melts calculated from mineral compositions demonstrate strong enrichments of incompatible elements relative to mare basalts. This geochemical signature closely matches that of KREEP, and has led to the conclusion that NWA 773 is a mixture of a magnesian magma and an extremely evolved KREEP-rich component[11]. Thus, NWA 773 has geochemical affinities to other

KREEP-rich samples such as the Mg-suite, alkali suite and the KREEP basalts.

We have completed Rb–Sr and Sm–Nd isotopic analyses on whole-rock and mineral fractions from the olivine clast in NWA 773. We obtained 100 mg of NWA 773 from the Natural History Museum, London. Our analytical procedures are described in the Methods section and are similar to those described by us previously[12]. The isotopic results are presented in Table 1 and Fig. 1. The whole-rock and mineral fractions (olivine, olivine + pyroxene and plagioclase) define a Sm–Nd isochron with an age of 2.865 ± 0.031 Gyr, using the Isoplot program[13]. Regression of the data resulted in a mean-squared weighted derivative (MSWD) of about one, indicating that all points lie within uncertainty of the isochron. As a result, the Sm–Nd age appears to be robust.

Our Sm–Nd age is concordant with the Ar–Ar age of ~2.91 Gyr reported for NWA 773 (ref. 14). However, whereas Ar–Ar ages commonly reflect resetting events associated with the formation of large lunar impact basins, Sm–Nd ages are likely to represent crystallization ages. Thus, the age of NWA 773 is confirmed to be the youngest crystallization age derived from any lunar sample, as previously included from the Ar–Ar age (ref. 14). Although ages of mare basalt units have been estimated to be as young as 1.2 Gyr from crater size–frequency distribution measurements[15], the youngest crystallization age previously determined for a lunar sample is ~3.1 Gyr (ref. 16), whereas the youngest crystallization of a KREEP-rich sample (labelled 15382) reported previously was 3.83 ± 0.02 Gyr ago[17]. The 2.865 ± 0.031-Gyr crystallization age of NWA 773 reported here therefore extends the range of dated lunar samples by about 250 million years (Myr), and the period of KREEP-magmatism by about 1 Gyr.

The Sm–Nd isochron defines an initial ε_{Nd} isotopic composition of -7.84 ± 0.22 ($\varepsilon_{Nd} = [^{143}Nd/^{144}Nd^{sample} \div ^{143}Nd/^{144}Nd^{CHURat2.865Gyrago} - 1] \times 10^4$), indicating the sample is derived from a strongly light-REE (LREE)-enriched source region (CHUR, chondritic uniform reservoir). The $^{147}Sm/^{144}Nd$ ratio calculated for the NWA 773 source region is 0.158, and is significantly more LREE-enriched than the source region for any other dated lunar rock (Fig. 2). Shih *et al.*[18] suggested that many samples with KREEP-rich geochemical signatures have Sm–Nd isotopic systematics indicative of derivation from a common source region ($^{147}Sm/^{144}Nd$ ratio is 0.181; Fig. 2). Northwest Africa 773 does not lie on this array and is therefore derived from the most evolved source region yet known (that is, with the largest KREEP component). Interestingly, the $^{147}Sm/^{144}Nd$ ratio of the NWA 773 source is very similar to the ratio estimated for the KREEP source
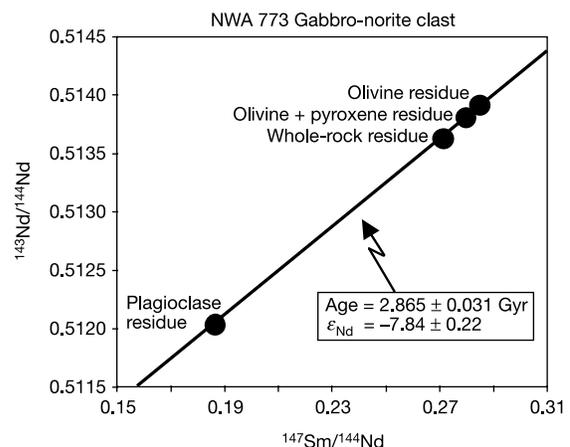

Figure 1 Sm–Nd isochron diagram for NWA 773, yielding the youngest lunar crystallization age of 2.865 ± 0.031 Gyr and the most negative ε_{Nd} value of -7.84 ± 0.22.

209

Table 1 Rb–Sr and Sm–Nd isotopic data for NWA 773

Fraction	Whole-rock residue	Plagioclase residue	Olivine + pyroxene residue	Olivine residue
Weight fraction (mg)	8.28	8.33	28.38	37.80
Rb (p.p.m.)	0.266	2.79	0.130	0.127
Sr (p.p.m.)	8.719	101.09	2.810	2.711
$^{87}Rb/^{86}Sr$*	0.08824 ± 44	0.07995 ± 40	0.13352 ± 67	0.13519 ± 68
$^{87}Sr/^{86}Sr$†	0.707849 ± 10	0.706845 ± 10	0.711716 ± 10	0.710068 ± 10
Sm (p.p.m.)	0.795	1.235	0.643	0.782
Nd (p.p.m.)	1.850	4.172	1.451	1.730
$^{147}Sm/^{144}Nd$‡	0.27085 ± 27	0.18661 ± 80	0.27922 ± 28	0.28494 ± 54
$^{143}Nd/^{144}Nd$§	0.513637 ± 10	0.512050 ± 10	0.513799 ± 10	0.513916 ± 11

NBS-987Sr standard ($N = 6$) = 0.710263 ± 16, La Jolla Nd standard ($N = 8$) = 0.512873 ± 14. Sr run on Re filaments with Ta_2O_5. Nd run as NdO at 5×10^{-7} torr.
*Error limits apply to last digits and include a minimum uncertainty of 0.5% plus 50% of the blank correction for Rb and Sr added quadratically.
†Normalized to $^{86}Sr/^{88}Sr$ = 0.1194. Uncertainties refer to last digits and are $2\sigma_m$, calculated from the measured isotopic ratios.
‡Error limits apply to last digits and include a minimum uncertainty of 0.1% plus 50% of the blank correction for Sm and Nd added quadratically.
§Normalized to $^{146}Nd/^{144}Nd$ = 0.7219. Uncertainties refer to last digits and are $2\sigma_m$, calculated from the measured isotopic ratios.

region[19]. This suggests that the KREEP source may be significantly more evolved than has been previously estimated.

The initial $^{87}Sr/^{86}Sr$ ratio of NWA 773 is estimated to be 0.703568 ± 0.000032 from the plagioclase mineral fraction using the Sm–Nd age. The $^{87}Rb/^{86}Sr$ ratio of the NWA 773 source region is calculated to be 0.195, assuming an initial $^{87}Sr/^{86}Sr$ ratio of BABI (best achondrite basalt initial) at 4.558 Gyr ago. This value is significantly higher than the values calculated for other KREEP-rich rocks, which are typically less than 0.05 (refs 18, 20), confirming that NWA 773 is derived from a more evolved source.

The presence of KREEP-rich material in the lunar mantle has long been viewed as a potential heat source for melting of mafic cumulates[4,6,7]. This stems from the observation that KREEP basalt has U and Th abundances that are enriched over chondrites by a factor of about 300 (ref. 4). The Rb/Sr ratios of the source regions of NWA 773 and other KREEP-rich samples have been calculated from their Rb–Sr isotopic systematics and plotted against age in Fig. 3. The Rb/Sr ratio of individual source regions is directly proportional to the amount of KREEP-rich material that they contain. For example, relatively KREEP-poor Apollo 15 glasses have low Rb/Sr ratios of about 0.014, whereas KREEP-rich mantle material has been estimated to have high Rb/Sr ratios of 0.11 (refs 4, 19, 21).

From Fig. 3 it is apparent that there is an inverse correlation between Rb/Sr ratio of the source region and the crystallization age. Samples with relatively old ages are derived from sources with low Rb/Sr ratios, whereas relatively young samples are derived from sources characterized by higher Rb/Sr ratios. Thus, the degree of incompatible element enrichment inferred for the source regions of individual samples (that is, the amount of KREEP-rich material present) increases as the samples become younger. This correlation could reflect the need for the source regions of young magmas to contain a greater abundance of heat-producing elements to offset cooling associated with heat loss of the Moon through time. This correlation provides evidence that the presence of KREEP-rich material in the source region may indeed be required to initiate melting.

The correlation between the abundance of KREEP in the source and age also suggests that Mg-rich cumulates and KREEP-rich material must be physically associated with one another in the source region for both heat and mass to be exchanged between Mg-rich cumulates and KREEP-rich components. Therefore, melting-differentiation models that require the assimilation of KREEP-rich material in shallow-level magma chambers by Mg-rich magmas derived from deep in the mantle are less feasible. Instead, it seems that KREEP-rich material is mixed with Mg-rich cumulates in the source region.

Alternatively, Snyder et al.[22,23] suggested that KREEP-rich samples from the Mg-suite and alkali suites were related by crystallization of closely related parental magmas. Several aspects of this model are consistent with the observation that young lunar samples have large KREEP geochemical signatures (Fig. 3). For example, the KREEP geochemical signature becomes more pronounced because the parental magma evolves through time. This, of course, requires KREEP-rich parental magmas to remain molten over the first 1.7 Gyr of lunar history. Although some thermal models predict KREEP-rich magmas to remain molten for very long periods of time[5,7], the Mg-rich nature of NWA773 is not consistent with this
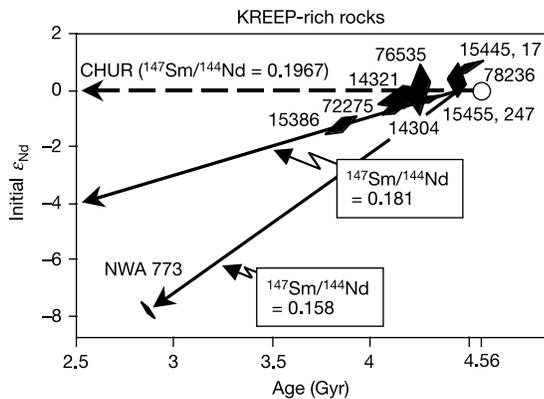

Figure 2 Age versus initial ε_{Nd} plot for KREEP-rich lunar rocks (Mg and alkali-suites, and KREEP basalts) demonstrating that NWA 773 is derived from the most evolved (LREE-enriched) lunar source region yet known. Data summary from refs 8 and 9. Solid lines are two-stage growth models for lunar source regions. The first stage represents growth in CHUR, between 4.558 Gyr ago and the time of magma ocean crystallization represented by the 4.42-Gyr KREEP model age. The second stage represents growth in the source regions of individual samples after 4.42 Gyr ago.
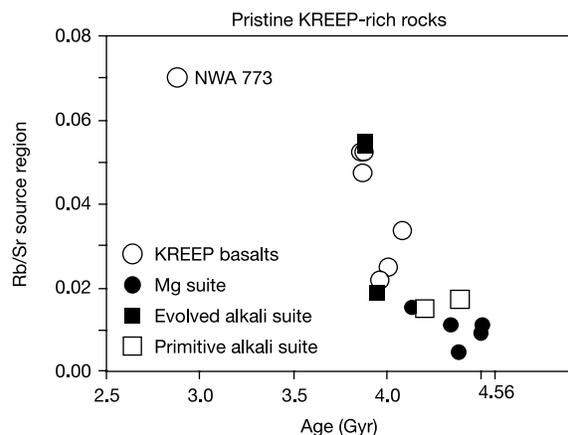

Figure 3 Plot of age versus Rb/Sr ratios of sample source regions calculated from their initial Sr isotopic compositions using a single-stage growth model. The inverse correlation suggests that KREEP is the heat source responsible for melting lunar samples.

hypothesis because it indicates that the parental magma is not particularly evolved.

There are two observations that are inconsistent with the hypothesis that KREEP initiates melting of mafic cumulates to produce young lunar magmas. First, there are no samples with ancient ages and large KREEP geochemical signatures in the sample collections. However, this could reflect a sampling bias introduced by the fact that all ancient KREEP-rich igneous samples are derived from two closely related plutonic suites[22]. The second observation is that radiometric ages determined on low- and high-Ti basalts that lack the KREEP geochemical signature are often relatively young (3.1 to 3.4 Gyr; refs 16, 24). This implies that another mechanism to melt sources with small amounts of KREEP-rich material is required. We speculate that KREEP-rich material is the heat source for these magmas as well. However, melting is not initiated at the site where this material resides; instead, heating of mafic cumulates by KREEP-rich materials promotes upwelling of diapirs in the mantle. Thus, melting could be initiated as pressure is released. If this mechanism is valid, it implies that KREEP-rich materials are directly or indirectly responsible for melting of the lunar mantle. □

Methods

The sample was washed and sonicated in four-times quartz-distilled water, followed by 0.5 M acetic acid. The sample was next crushed using a sapphire mortar and pestle, and sieved at 100–200 and 200–325 mesh. Mineral separations were begun using heavy liquids on both size fractions. Plagioclase floated in 2.85 g cm^{-3}, whereas the mafic minerals sank. Hand-picking was used to separate pyroxene (brown) and olivine (green) mineral grains, as well as to purify the plagioclase fraction. Individual mineral fractions were then leached in 1 N HCl for 10 min in a sonicator before digestion. Chemical separations and isotope ratio measurements were done at the Radiogenic Isotope Laboratory, University of New Mexico, following standard silicate dissolution procedures, and involved cation chromatography using a combination of HCl and methalactic acids. Isotopic ratios were measured on a Micromass Sector 54 multi-collector thermal ionization mass spectrometer on Faraday cups in static mode. Rubidium, Sr, Sm, and Nd blanks measured during the course of the investigation averaged 7, 12, 7 and 8 pg, respectively. Normalization and standard values are given in Table 1.

1. Wood, J. A., Dickey, J. S., Marvin, U. B. & Powell, B. N. Lunar anorthosites and a geophysical model of the Moon. *Proc. 1st Lunar Planet. Sci. Conf.* 965–988 (Pergamon, New York, 1970).

2. Smith, J. A., *et al.* Petrologic history of the Moon inferred from petrography, mineralogy, and petrogenesis of Apollo 11 rocks. *Proc. 1st Lunar Planet. Sci. Conf.* 1149–1162 (Pergamon, New York, 1970).

3. Snyder, G. A., Taylor, L. A. & Neal, C. R. A chemical model for generating the sources of mare basalts: Combined equilibrium and fractional crystallization of the lunar magmasphere. *Geochim. Cosmochim. Acta* 56, 3809–3823 (1992).

4. Warren, P. H. & Wasson, J. T. The origin of KREEP. *Rev. Geophys. Space Phys.* 17, 73–88 (1979).

5. Warren, P. H. The origin of pristine KREEP: Effects of mixing between urKREEP and the magmas parental to the Mg-rich cumulates. *Proc. 8th Lunar Planet. Sci. Conf.* 233–241 (1988).

6. Hess, P. C. & Parmentier, E. M. Thermal evolution of a thicker KREEP liquid layer. *J. Geophys. Res.* 106, 28023–28032 (2001).

7. Wieczorek, M. A. & Phillips, R. J. The "Procellarum KREEP Terrane": Implications for mare volcanism and lunar evolution. *J. Geophys. Res.* 105, 20417–20430 (2000).

8. Nyquist, L. E. & Shih, C.-Y. The isotopic record of lunar volcanism. *Geochim. Cosmochim. Acta* 56, 2213–2234 (1992).

9. Snyder, G. A., Borg, L. E., Nyquist, L. E. & Taylor, L. A. in *Chronology and Isotopic Constraints on Lunar Evolution* (eds Canup, R. & Righter, K.) 361–395 (Univ. Ariz. Press, Tucson, 2000).

10. Fagan, T. J. *et al.* Northwest Africa 773: Lunar origin and iron-enrichment trend. *Meteorit. Planet. Sci.* 38, 529–554 (2003).

11. Jolliff, B. L., Korotev, R. L., Zeigler, R. A. & Floss, C. Northwest Africa 773: Lunar mare breccia with a shallow-formed olivine-cumulate component, very low Ti (VLT) heritage and a KREEP connection. *Geochim. Cosmochim. Acta* 67, 4857–4879 (2003).

12. Borg, L. E., Nyquist, L. E., Weismann, H., Shih, C.-Y. & Reese, Y. The age of Dar al Gani 476 and the differentiation history of the martian meteorites inferred from their radiogenic isotopic systematics. *Geochim. Cosmochim. Acta* 67, 3519–3536 (2003).

13. Ludwig, K. J. R. *Users Manual for Isoplot/Ex v. 2.49: A Geochronological Toolkit for Microsoft Excel* (Berkeley Geochronology Center Special Publication No. 1a, BGC, Berkeley, 2001) ⟨http://www.bgc.org/klprogrammenu.html⟩.

14. Fernandes, V. A., Burgess, R. & Turner, G. ^{40}Ar-^{39}Ar chronology of lunar meteorites Northwest Africa 032 and 773. *Meteorit. Planet. Sci.* 38, 555–564 (2003).

15. Hiesinger, H., Head, J. W., Wolf, U., Jaumann, R. & Neukum, G. Ages and stratigraphy of mare basalts in Oceanus Procellarum, Mare Nubium, Mare Cognitum, and Mare Insularum. *J. Geophys. Res.* 108, 1–27 (2003).

16. Nyquist, L. E., Bansal, B. M., Wooden, J. L. & Wiesmann, H. Sr-isotopic constraints on the petrogenesis of Apollo 12 basalts. *Proc. 8th Lunar Planet. Sci. Conf.* 1383–1415 (Pergamon, New York, 1977).

17. Papanastassiou, D. A. & Wasserburg, G. J. Rb-Sr age of troctolite 76535. *Proc. 7th Lunar Sci. Conf.* 2035–2054 (Pergamon, New York, 1976).

18. Shih, C.-Y. *et al.* Age of pristine noritic clasts from lunar breccias 15445 and 15455. *Geochim. Cosmochim. Acta* 57, 915–931 (1993).

19. Warren, P. H. in *Workshop on Moon in Transition: Apollo 14, KREEP, and Evolved Lunar Rocks* 149–153 (LPI Technical Report 98–03, Lunar and Planetary Institute, Houston, 1989).

20. Shih, C.-Y., Nyquist, L. E., Bansal, B. M. & Weismann, H. Rb-Sr and Sm-Nd chronology of an Apollo 17 KREEP basalt. *Earth Planet. Sci. Lett.* 108, 203–215 (1992).

21. Hughes, S. S., Delano, J. W. & Schmitt, R. A. Apollo 15 yellow-brown glass: Chemistry and petrogenetic relations to green volcanic glass and olivine-normative basalts. *Geochim. Cosmochim. Acta* 52, 2379–2391 (1988).

22. Snyder, G. A., Taylor, L. A. & Halliday, A. N. Chronology and petrogenesis of the lunar highlands alkali suite: Cumulates from KREEP basalt crystallization. *Geochim. Cosmochim. Acta* 59, 1185–1203 (1995).

23. Snyder, G. A., Neal, C. R., Taylor, L. A. & Halliday, A. N. Processes involved in the formation of magnesian-suite plutonic rocks from the highlands of the Earth's moon. *J. Geophys. Res.* 100, 9365–9388 (1995).

24. Dash, E. J. *et al.* Time of crystallization of a unique A15 basalt. *Lunar Planet. Sci. Conf.* XX, 218–219 (1989).

....

Nonindependence of mammalian dental characters

Aapo T. Kangas, Alistair R. Evans, Irma Thesleff & Jukka Jernvall

Developmental Biology Program, Institute of Biotechnology, PO Box 56, FIN-00014, University of Helsinki, Helsinki, Finland

....

Studies of mammalian evolution frequently use data derived from the dentition[1–4]. Dental characters are particularly central for inferring phylogenetic relationships of fossil taxa[1–4], of which teeth are often the only recovered part. The use of different aspects of dental morphology as phylogenetic signals implies the independence of dental characters from each other. Here we report, however, that, at least developmentally, most dental characters may be nonindependent. We investigated how three different levels of the cell signalling protein ectodysplasin (Eda)[5] changed dental characters in mouse. We found that with increasing expression levels of this one gene, the number of cusps increases, cusp shapes and positions change, longitudinal crests form, and number of teeth increases. The consistent modification of characters related to lateral placement of cusps can be traced to a small difference in the formation of an early signalling centre at the onset of tooth crown formation. Our results suggest that most aspects of tooth shape have the developmental potential for correlated changes during evolution which may, if not taken into account, obscure phylogenetic history.

Although both new fossil and molecular data can be expected to resolve many of the phylogenetic incongruences[6–10], there is a continuing debate about the best way to use dental evidence in evolutionary taxonomy[6,9,10]. The 'total evidence' view assumes that covarying characters manifest phylogenetic congruence, but other views assume that covariance of characters can be misinterpreted as a phylogenetic signal for functional or developmental reasons. As part of the same individual ontogeny, all characters obviously have the potential for nonindependent, or correlated, changes during evolution, but whether this could be the case for most mammalian dental characters used in evolutionary taxonomy remains unresolved. Features of the mammalian dentition, as part